Research in Astronomy and Astrophysics manuscript no.
(LaTeX: raa23b.tex; printed on June 6, 2023; 1:05)

New cases of super-flares on slowly rotating solar-type stars and large amplitude super-flares in G- and M-type main-sequence stars.

A. k. Althukair[1,2] and D. Tsiklauri[1]

[1] Department of Physics and Astronomy, School of Physical and Chemical Sciences, Queen Mary University of London, Mile End Road, London, E1 4NS, UK; *a.k.althukair@qmul.ac.uk*, *d.tsiklauri@qmul.ac.uk*

[2] Physics Department, College of Sciences, Princess Nourah Bint Abdulrahman University, Riyadh, PO Box 84428, Saudi Arabia

Received 20xx month day; accepted 20xx month day

Abstract In our previous work, we searched for super-flares on different types of stars while focusing on G-type dwarfs using entire Kepler data to study statistical properties of the occurrence rate of super-flares. Using these new data, as a by-product, we found fourteen cases of super-flare detection on thirteen slowly rotating Sun-like stars with rotation periods of 24.5 to 44 days. This result supports earlier conclusion by others that the Sun may possibly have a surprise super-flare. Moreover, we found twelve and seven new cases of detection of exceptionally large amplitude super-flares on six and four main-sequence stars of G- and M-type, respectively. No large-amplitude flares were detected in A, F, or K main-sequence stars. Here we present preliminary analysis of these cases. The super-flare detection, i.e. an estimation of flare energy, is based on a more accurate method compared to previous studies. We fit an exponential decay function to flare light curves and study the relation between e-folding decay time, τ, vs. flare amplitude and flare energy. We find that for slowly rotating Sun-like stars, large values of τ correspond to small flare energies and small values of τ correspond to high flare energies considered. Similarly, τ is large for small flare amplitudes and τ is small for large amplitudes considered. However, there is no clear relation between these parameters for large amplitude super-flares in the main sequence G- and M-type stars, as we could not establish clear functional dependence between the parameters via standard fitting algorithms.

Key words: stars: activity — stars: flare — stars: rotation — stars: solar-type — stars: statistics — Sun: flares

It is believed the Solar and stellar flares are powered by a physical process called magnetic reconnection, 1994; Shibata et al. 1995). This is accompanied by acceleration of plasma particles and release of heat. The source of this kinetic and thermal energy is the energy stored in the magnetic field. Thus, the magnetic dynamo process which is one of possible means to generate magnetic field via bulk plasma flows is of great importance for understanding of what can power and therefore be source for a flare or a super-flare. The energies of observed stellar flares lie in the wide range from 10^{28} to 10^{37} erg, while the highest energy of any observed solar flare is approximately few times 10^{32} erg. Thus, generally agreed terminology is that a super-flare should have an energy in excess of 10^{34} erg. A plausible dynamo model capable to explain the generation of magnetic energy sufficient to support super-flares has been recently suggested in Kitchatinov & Olemskoy (2016) and then further investigated in Katsova et al. (2018). In this scenario, rather than producing stellar cycles similar to the solar 11 year cycle, the dynamos in superflaring stars excite some quasi-stationary magnetic configuration with a much higher magnetic energy. Further, Kitchatinov et al. (2018) used a flux-transport model for the solar dynamo with fluctuations of the Babcock-Leighton type α-effect to generate statistics of magnetic cycles. As a result, they concluded that the statistics of the computed energies of the cycles suggest that super-flares with energies in excess of 10^{34} erg are not possible on the Sun.

Historical records suggest that no super-flares have occurred on the Sun in the last two millennia. In the past there were notable examples detection of super-flares on Sun-like stars. There are two references which support such clam Schaefer et al. (2000) and Nogami et al. (2014).

As claimed by Schaefer et al. (2000) they identified nine cases of super-flares involving 10^{33} to 10^{38} ergs on main sequence Sun-like stars. Sun-like means that stars are on or near the main-sequence, have spectral class from F8 to G8, are single (or have a very distant binary companion). The super-flare energy estimation by Schaefer et al. (2000) was based on photometric methods.

Nogami et al. (2014) reported the results of high dispersion spectroscopy of two 'super-flare stars', KIC 9766237, and KIC 9944137 using Subaru/HDS telescope. These two stars are G-type main sequence stars, and have rotation periods of 21.8 days, and 25.3 days, respectively. Their spectroscopic results confirmed that these stars have stellar parameters similar to those of the Sun in terms of the effective temperature, surface gravity, and metallicity. By using the absorption line of Ca II 8542, the average strength of the magnetic field on the surface of these stars was estimated to be 1-20 G. The super-flare energy estimation by Nogami et al. (2014) was based semi-empirical method based on magnetic energy density times volume of flare. These results claim that the spectroscopic properties of these super-flare stars are very close to those of the Sun, and support the hypothesis that the Sun may have a super-flare.

Statistical study of super-flares on different stellar types has been an active area of research (Maehara et al. 2012; Shibayama et al. 2013; Wu et al. 2015; He et al. 2015, 2018; Yang et al. 2017; Van Doorsselaere et al. 2017; Lu et al. 2019; Yang & Liu 2019; Günther et al. 2020; Tu et al. 2020; Gao et al. 2022). Shibayama et al. (2013) studied statistics of stellar super-flares. These authors discovered that for Sun-like stars (with surface temperature 5600-6000 K and slowly rotating with periods longer than 10 days), the occurrence rate of super-flares with an energy of $10^{34} - 10^{35}$ erg is once in 800-5000 yr. Shibayama et al. (2013) confirmed the previous results of Maehara et al. (2012) in that the occurrence rate (dN/dE) of super-flares rate distribution versus flare energy is roughly similar to that for solar flares. Tu et al. (2020) identified and verified 1216 super-flares on 400 solar-type stars by analyzing 2-minute cadence data from 25,734 stars observed during the first year of the TESS mission. The results indicate a higher frequency distribution of super-flares compared to the findings from the Kepler mission. This difference may be due to a significant portion of the TESS solar-type stars in the dataset are rapidly rotating stars. The power-law index γ of the super-flare frequency distribution was determined to be $\gamma = 2.16 \pm 0.10$, which is consistent with the results obtained from the Kepler mission. The study highlights an extraordinary star, TIC43472154, which exhibits approximately 200 super-flares per year. Tu et al. (2020) analyzed the correlation between the energy and duration of super-flares, represented as $T_{duration} \propto E^{\beta}$. They derived a power-law index $\beta = 0.42 \pm 0.01$ for this correlation, which is slightly larger than the value of $\beta = 1/3$ predicted by magnetic reconnection theory. We believe that method for flare energy estimation used in (Shibayama et al. 2013; Yang et al. 2017) is more accurate than one used by Schaefer et al. (2000) and Nogami et al. (2014). We therefore base of flare energy estimate on method of Shibayama et al. (2013) and Althukair & Tsiklauri (2022) referred thereafter as Paper I.

In Paper I we searched for super-flares on different spectral class stars, while focusing on G-type dwarfs (solar-type stars) using Kepler data using quarters $0 - 17$ with the purpose of study the statistical properties of the occurrence rate of super-flares. Shibayama et al. (2013) studied statistics of stellar super-flares based on Kepler data in quarters $0 - 6$ ($Q0 - Q6$). In Paper I we investigated how the results are modified by adding more quarters, i.e. what is α power-law for data quarters $0 - 17$ and $7 - 17$. Here using the more extended Kepler data, we also found 14 cases of detection of Super-flares on 13 Slowly Rotating Sun-like starts in each of KIC 3124010, KIC 3968932, KIC 7459381, KIC 7459381, KIC 7821531, KIC 9142489, KIC 9528212, KIC 9963105, KIC 10275962, KIC 11086906, KIC 11199277, KIC 11350663 and KIC 11971032. Thus the main purpose of the present study is to present analysis of these new 14 cases. The main novelty here is that the detection is based on a Shibayama et al. (2013) method, which is more accurate, as compared to Schaefer et al. (2000) and Nogami et al. (2014) for the flare energy estimation. Our results support earlier conclusion by others (Schaefer et al. (2000) and Nogami et al. (2014)) that the Sun may have a surprise super-flare. We stress that Paper I has conducted a more comprehensive study of determination of stellar rotation periods based on a robust method such as used by McQuillan et al. (2014) in comparison to Shibayama et al. (2013). We believe that more accurate period determination used in Paper I has led to the current new results, presented in this paper. In addition to the 14 cases of of Super-flares on Slowly Rotating Sun-like starts, we detected 12 and 7 super-flares with a large amplitude on five G-type and four M-type main sequence stars, respectively.

Solar flares emit energy at all wavelengths, but their spectral distribution is still unknown. When white-light continuum emission is observed, the flares are referred to as ”white-light flares” (WLF). Kretzschmar (2011) identified and examined visible light emitted by solar flares and found that the white light is present on average during all flares and must be regarded as a continuum emission. Kretzschmar (2011) also demonstrated that this emission is consistent with a black body spectrum with temperature of 9000 K and that the energy of the continuum contains roughly 70% of the total energy emitted by the flares. WLFs are among flare's EUV or soft X-ray luminosity reaches a reasonably large threshold (McIntosh & Donnelly 1972; Neidig & Cliver 1983). Thus, optical continuum is presumably present in all flares but only in a few cases it reaches a measurable degree of brightness. This conclusion implies that WLFs are not fundamentally different from conventional flares Neidig (1989). Nonetheless, WLFs are important in flare studies because they are similar to stellar flares ways Worden (1983) and because they represent the most extreme conditions encountered in solar optical flares Neidig (1989). Using observations from the Transiting Exoplanet Survey Satellite (TESS), Ilin et al. (2021) present four fully convective stars that exhibited white light flares of large size and long duration. The underlying flare amplitude as a fraction of the quiescent flux of two flares is greater than two. After the discovery of the largest amplitude flares ever recorded on the L0 dwarf, which reached $\Delta V \approx -11$ magnitude Schmidt et al. (2016), Jackman et al. (2019) detected a large amplitude white-light super-flare on the L2.5 dwarf ULAS J224940.13011236.9 with the flux $\Delta V \approx -10$ magnitude which corresponds to a relative brightness ratio of 10000. This can be demonstrated as follows:

$$\Delta V = V_{\max} - V_{\min} \approx -10, \tag{1}$$

where $V_{\max}$ is the apparent magnitude in the visible band corresponding to the flux at the maximum amplitude ($F_{\max}$), and $V_{\min}$ is the apparent magnitude in the visible band corresponding to the flux at the minimum state ($F_{\min}$). Using the magnitude difference calculation :

$$V_{\max} - V_{\min} = -10 = 2.5 \log_{10}(F_{\min}/F_{\max}), \tag{2}$$

it is clear that $F_{\max}/F_{\min} = \Delta F/F = 10000$.

Here we present the detection of 14 super-flares on 13 slowly-rotating Sun-like stars, 12 and 7 cases of large amplitude super-flares on five G-type dwarfs and four M-type dwarfs respectively. Section 1 presents the method used including the flare detection, the flare energy estimation, and rotation period determination. Section 2 provides the main results of this study. Section 3 closes this work by providing our main conclusions.

1 METHODS

1.1 Flare Detection

We conducted an automated search for super-flares on main-sequence stars type (A, F, G, K, M) based on entire Kepler data, using our Python script on long cadence data from Data Release 25 (DR 25) following (Maehara et al. 2012; Shibayama et al. 2013) method. The parameters for all targets observed by Kepler have been taken from the Kepler Stellar interactive table in NASA Exoplanet Archive. The study was carried out on a sample of main sequence stars, comprising 2222, 10307, 25442, 10898, and 2653 stars for the spectral types of M, K, G, F, and A, respectively. The following is a brief description of this method. We generate light curves of the stars using the PDCSAP flux. Then, in order to be statistically precise, we computed the distributions of brightness variation by calculating the flux difference in adjacent time intervals between every two neighboring data points in the light curve. Then, we determine the flux difference value at which the area under the distribution equals 1% of the total area. In order to increase the threshold, the 1% value

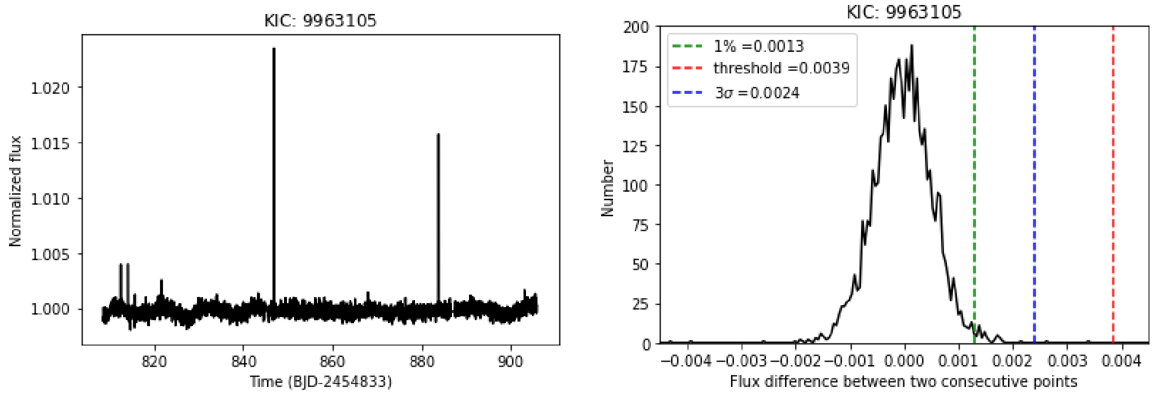

Fig. 1: Illustrations of flares detection method used by Shibayama et al. (2013). (a) The light curve of KIC 9963105. (b) The distribution of brightness variation between each pair of adjacent data points in the light curves of KIC 9963105. The green vertical line represents the value of 1% of the total area under the curve, the red vertical lines represents the flare detection threshold and the blue vertical represents 3σ of the brightness variation distribution.

the flux difference between two consecutive points exceeded the threshold for the first time. To determine the end time of the flare, we computed the three standard deviations 3σ of the distribution of brightness variation. Figure 1 displays a typical results for this method for KIC 9963105. The light curve of KIC 9963105 are shown in Figure 1(a). Figure 1(b) shows the distribution of the brightness difference between every two adjacent data points of KIC 9963105 light curve. 1% of the total area under the distribution curve is represented by the green vertical line. The red vertical line represents the flare detection threshold value, which is equal to three times 1% value of the area under the distribution curve. The blue vertical line is 3σ of the distribution of the brightness variation. To determine the flare end time, we fit a B-spline curve through three points on the relative flux ($\Delta F/F_{\rm avg}$) distributed around the flare. One point just before the flare, and the other two points five and eight hours after the flare peak, respectively. Then we subtract the B-spline curve from the relative flux in order to remove long-term brightness variations around the flare Shibayama et al. (2013). We define the flare end time as the time when the relative flux produced by the subtraction drops below the value of 3σ for the first time. After detecting flare events, conditions were applied to all flare candidates. These conditions are: the flare duration must exceed 0.05 days, corresponding to at least three data points two of them after the flare peak, and the flare's decline phase must be longer than its rising phase Shibayama et al. (2013). Only flare incidents meeting these criteria were analysed.

1.2 Energy Calculation

Schaefer et al. (2000) identified nine cases of super-fares involving $10^{33} - 10^{38}$ ergs on normal solar-type stars. Their super-flare energy estimate has a large uncertainty, e.g. Groombridge 1830 (HR 4550) total flare energy (in the blue band alone) is 10^{35} ergs with an uncertainty of a factor of a few due to having only four points on the light curve.

The possibility that super-flares can be explained by magnetic energy stored on the star's surface was considered by Nogami et al. (2014) Using the Ca ii 8542 absorption line, they estimate that the average targets has a total energy of 10^{34} erg. Under the assumption that the energy released during the flare represents a fraction (f) of the magnetic energy stored around the spot area. Their flare energy ($E_{\rm flare}$) was calculated as follows:

$$E_{\rm flare} \sim f\frac{B^2}{8\pi}L^3. \quad (3)$$

The length of the magnetic structure causing the flare (L), has been considered to be the same size as the spotted region, i.e. $L = \sqrt{a\pi R_*^2}$ where a is the spot's area, which giving that

$$E_{\rm flare} \sim f\frac{B^2}{8\pi}(a\pi R_*^2)^{3/2}. \quad (4)$$

Our energy estimation for each flare depends on the star's luminosity ($L_{\rm star}$), flare amplitude ($f_{\rm amp}$), and flare duration (Shibayama et al. 2013; Yang et al. 2017). $L_{\rm star}$, the amount of energy that the star emits in one second, is proportional to the star's radius R squared and its surface temperature $T_{\rm eff}$ to the fourth power, and is obtained from the following equation:

$$L_{\rm star} = \sigma_{\rm SB}T_{\rm eff}^4 4\pi R^2, \quad (5)$$

where $\sigma_{\rm SB}$ is the Stefan-Boltzmann constant, $4\pi R^2$ is the entire surface area of the star. The continuum emission from a white-light flare is consistent with blackbody radiation at around 9000 K, as suggested by (Hawley & Fisher 1992; Kretzschmar 2011). Based on (Shibayama et al. 2013; Yang et al. 2017; Günther et al. 2020), we set $T_{\rm flare}$ = 9000 K and derive the luminosity of a blackbody-emitting star as follows:

$$L_{\rm flare}(t) = \sigma_{\rm SB}T_{\rm flare}^4 A_{\rm flare}, \quad (6)$$

where $A_{\rm flare}$ is the flare's area, as determined by the formula:

$$A_{\rm flare}(t) = f_{\rm amp}(t)\pi R^2\frac{\int R_\lambda B_\lambda(T_{\rm eff})d\lambda}{\int R_\lambda B_\lambda(T_{\rm flare})d\lambda}, \quad (7)$$

where $f_{\rm amp}$ represents the flare amplitude for the relative flux and R_λ represents the Kepler instrument's response function Caldwell et al. (2010). The Kepler photometer covers various wavelengths, from 420 to 900 nm. The Plank function at a specific wavelength, denoted by $B_\lambda(T)$, is given by:

$$B_\lambda(T) = \frac{2hc^2/\lambda^5}{e^{hc/\lambda kT}-1}, \quad (8)$$

where h represents Planck's constant, c the speed of light, T the black body temperature, and k Boltzmann's constant. By substituting Eq.(7) into (6), we calculate the total flare energy by the integral of $L_{\rm flare}$ over the flare duration :

$$E_{\rm flare} = \int_{t_{\rm start}}^{t_{\rm end}} L_{\rm flare}(t)dt. \quad (9)$$

1.3 Rotational Period Determination

Light curve periods were calculated using the Lomb-Scargle periodogram, a common statistical approach for detecting and characterising periodic signals in sparsely sampled data. We used an oversampling factor of five VanderPlas (2018), and use PDCSAP flux to generate a Lomb-Scargle periodogram for each light curve from Q2 to Q16. Furthermore, the period corresponding to the maximum power of the periodogram was allocated as the rotation period for the Kepler ID in a specific quarter. This value was estimated with an the results, allowing us to automate the selection of the star's rotation period rather than manually. We set 0.5 days for periods shorter than a day and eliminated periods less than 0.1 days. Finally, for each Kepler ID, we choose the most frequent period across all quarters from Q2 to Q16. Following the McQuillan et al. (2014) technique, we required that the period chosen for all quarters be identified in at least two unique segments, with the segment defined as three consecutive Kepler quarters. (Q2,Q3,Q4), (Q5, Q6, Q7), (Q8, Q9, Q10), (Q11, Q12, Q13) and (Q14,Q15,Q16).

2 RESULTS

By performing an automated search for super-flares on G-type main-sequence stars during 1442 days of Kepler observation in all of (DR 25) long-cadence data from Q0 to Q17, we found 14 super-flares on 13 slowly rotating Sun-like stars in each of (KIC 3124010, KIC 3968932, KIC 7459381, KIC 7459381, KIC 7821531, KIC 9142489, KIC 9528212, KIC 9963105, KIC 10275962, KIC 11086906, KIC 11199277, KIC 11350663 and KIC 11971032), with a surface temperature of $5600K \leqslant T_{\rm eff} < 6000K$, a surface gravity of $\log\ g > 4.0$, and a rotational period $P_{\rm rot}$ range between 24.5 to 44 days. Figure 2 shows seven light curves of these events. The left panels display light curves over a 90-day of observation. The blue arrow on the left panel indicates the observed super-flare, which met all conditions. The right panels show zoomed in time light curves of super-flares. The blue squares represent the data points for a super-flare. We fitted an exponential decay function to the flare light curve to characterise the flares, shown by a red dashed curve. This exponential decay function is given by:

$$f(t) = a\ e^{-t/\tau} + b \tag{10}$$

where $f(t)$ is the relative flux as a function of time, a is the flare peak height, which is approximately equal to the relative flux at the flare peak, b is the relative flux in the quiescent state and τ is the decay time of the flare, which is the time at which the relative flux is decreased to $1/e \simeq 0.3679$ of its initial value. The value of τ, a and b of the exponential decay function for each flare are shown in the right panel. Flare parameters and their duration, amplitudes, energies and τ values are listed in Table 1. The rotation periods for these slowly rotating Sun-like stars were taken from McQuillan et al. (2014). Their flare energies range from $(1.9 - 9.0) \times 10^{34}$ erg. The flare amplitude of the slowly rotating Sun-like stars is relatively small, ranging between 0.002 and 0.018. We also find that the duration of flares in all of these cases is the same 0.061 days. This is probably due to the fact that flare duration of all small amplitude super-flares is two data points in time or *less*. Therefore, because one of the flare detection conditions in our code is that there must be at least two data points between the flare's peak and the end, cases with flare duration less than two points were not detected, and we end up with the same duration super-flares with the two data points. Because it appears that there are no small amplitude super-flares with duration *greater* than two data points, all flare duration end up the same. This selection effect is because we use long cadence light curve data, which has a 29.4-minute interval between each data point in time. The value of τ varies from 0.012 to 0.036 days.

In addition to the 14 cases of of super-flares on slowly rotating Sun-like starts, we detected 12 super-flares with a large amplitude on 6 G-type dwarfs in each of KIC 5865248, KIC 6783223, KIC 7505473, KIC 10053146, KIC 10057002 and KIC 11709752. Figure 3 shows eight light curves of these events same

Table 1: super-flares on slowly rotating Sun-like stars.

Kepler ID	$\mathrm{T_{eff}}$ (K)	log g	Radius $(R_\odot)$	P_{rot}[a] (day)	$\mathrm{t_{start}}$ (BJD)	$\mathrm{t_{end}}$ (BJD)	$\mathrm{t_{peak}}$ (BJD)	amp	Flare Duration (day)	τ (day)	Flare Energy (erg)
3124010	5688	4.46	1.01	25.90	913.24	913.30	913.26	0.008	0.061	0.017	4.57×10^{34}
3968932	5716	4.39	0.96	24.56	868.88	868.94	868.90	0.004	0.061	0.026	3.89×10^{34}
7459381	5635	4.27	1.11	26.19	312.31	312.37	312.33	0.005	0.061	0.017	4.89×10^{34}
7668358	5668	4.36	0.98	41.83	841.13	841.19	841.15	0.003	0.061	0.030	1.94×10^{34}
7821531	5681	4.52	0.92	32.66	891.81	891.87	891.83	0.018	0.061	0.015	8.63×10^{34}
9142489	5878	4.51	0.95	25.20	1561.13	1561.19	1561.15	0.004	0.061	0.028	2.61×10^{34}
9528212	5872	4.42	0.97	61.43	1332.34	1332.40	1332.36	0.003	0.061	0.036	2.31×10^{34}
9963105	5751	4.39	1.01	28.09	883.80	883.86	883.82	0.016	0.061	0.012	9.00×10^{34}
10275962	5782	4.51	0.91	26.12	213.21	213.27	213.23	0.007	0.061	0.035	3.71×10^{34}
10275962	5782	4.51	0.91	26.12	599.85	599.91	599.87	0.004	0.061	0.029	2.04×10^{34}
11086906	5758	4.38	1.11	29.18	1206.01	1206.07	1206.03	0.002	0.061	0.018	1.90×10^{34}
11199277	5638	4.49	0.92	29.00	325.43	325.49	325.45	0.008	0.061	0.029	3.72×10^{34}
11350663	5966	4.49	0.96	36.92	1232.31	1232.37	1232.33	0.010	0.061	0.014	5.21×10^{34}
11971032	5942	4.51	0.94	44.00	1231.92	1231.98	1231.94	0.006	0.061	0.030	3.80×10^{34}

[a] Rotation period from McQuillan et al. (2014).

parameters. The energy of their flares range from 1.67×10^{36} to 1.42×10^{38} erg. The rotation period of KIC 1170952 was obtained by this work. As for the rotation period for the other five stars, no such data is available. Even applying the method described in Paper I does not allow period determination in these five cases. According to Yang et al. (2017), there are three possible reasons: (i) due to the inclination angle and low activity level, the light curve has a small amplitude at the accuracy level of Kepler; (ii) fast-rotating stars have spots in the poles Schüssler & Solanki (1992), making it hard to detect light variation through rotation; and (iii) the rotation period is longer than 90 days (a quarter), making it difficult (or impossible) to detect them in the frequency spectrum of the star. The flare amplitude for these cases range between 4.05 and 35.60. These flares tend to last longer than flares with smaller amplitude of slowly rotating Sun-like stars as their duration varies between 0.061 and 0.143 day. The τ values of flares exhibiting large amplitude on G-type main-sequence stars are observed to be higher than those of flares occurring on slowly rotating Sun-like stars, as their values range between 0.014 and 0.058 days.

Table 2: Large amplitude super-flares on G-type main-sequence stars.

Kepler ID	$\mathrm{T_{eff}}$ (K)	log g	Radius $(R_\odot)$	P_{rot}[a] (day)	$\mathrm{t_{start}}$ (BJD)	$\mathrm{t_{end}}$ (BJD)	$\mathrm{t_{peak}}$ (BJD)	amp	Flare Duration (day)	τ (day)	Flare Energy (erg)
5865248	5780	4.44	1	NA	1476.22	1476.33	1476.24	13.16	0.102	0.036	7.29×10^{37}
5865248	5780	4.44	1	NA	1496.09	1496.21	1496.11	8.78	0.123	0.041	9.56×10^{37}
5865248	5780	4.44	1	NA	1561.78	1561.86	1561.80	8.14	0.082	0.034	6.75×10^{37}
6783223	5780	4.44	1	NA	1510.76	1510.86	1510.78	35.60	0.102	0.030	8.6×10^{37}
7505473	5780	4.44	1	NA	1385.81	1385.95	1385.85	4.05	0.143	0.058	1.67×10^{36}
10053146	5780	4.44	1	NA	1411.27	1411.33	1411.29	22.75	0.061	0.040	1.42×10^{38}
10057002	5780	4.44	1	NA	1284.52	1284.58	1284.54	12.03	0.061	0.049	6.24×10^{37}
11709752	5780	4.44	1	0.5	1501.56	1501.62	1501.58	4.21	0.061	0.031	2.85×10^{37}
11709752	5780	4.44	1	0.5	1544.06	1544.13	1544.08	7.65	0.061	0.014	2.85×10^{37}
11709752	5780	4.44	1	0.5	1571.49	1571.55	1571.51	4.48	0.061	0.033	3.94×10^{37}
11709752	5780	4.44	1	0.5	1575.35	1575.43	1575.37	5.11	0.082	0.046	5.44×10^{37}
11709752	5780	4.44	1	0.5	1578.39	1578.45	1578.41	9.40	0.061	0.030	3.94×10^{37}

[a] Rotation period from (Althukair & Tsiklauri 2023)

For stars of other spectral classes, no significant flares with large amplitudes were detected on main-sequence stars of type A, F, and K. Only M-type main-sequence stars manifested seven super-flares with large amplitude on each of KIC 6580019, KIC 7123391, KIC 7341517 and KIC 9201463. Similar to Figures 2 and 3, Figure 4 displays the seven light curves for these events. The parameters of these super-flares, including their duration, amplitude, energy, and τ values, are displayed in Table 3. These flares have an energy between 3.16×10^{33} and 1.59×10^{35} erg, amplitude ranges between 3.91 and 15.14 and their duration lasts between 0.018 and 0.044 day. τ values for super-flares with large amplitude on M-type main sequence stars vary from 0.030 to 0.049 days.

Table 3: Large amplitude super-flares on M-type main-sequence stars.

Kepler ID	T_{eff} (K)	log g	Radius ($R_\odot$)	P_{rot} (day)	t_{start} (BJD)	t_{end} (BJD)	t_{peak} (BJD)	amp	Flare Duration (day)	τ (day)	Flare Energy (erg)
6580019	2661	5.28	0.12	NA	609.97	610.09	609.99	3.91	0.123	0.044	7.04×10^{33}
6580019	2661	5.28	0.12	NA	674.45	674.60	674.47	10.30	0.143	0.041	1.25×10^{34}
7123391	3326	5.12	0.19	NA	638.53	638.59	638.55	8.07	0.061	0.038	4.76×10^{34}
7123391	3326	5.12	0.19	NA	692.09	692.19	692.13	12.38	0.102	0.018	1.23×10^{35}
7123391	3326	5.12	0.19	NA	794.54	794.72	794.56	15.14	0.184	0.049	1.59×10^{35}
7341517	2661	5.28	0.12	NA	877.95	878.12	877.99	5.27	0.163	0.041	4.82×10^{33}
9201463	3319	5.14	0.18	NA	215.11	215.27	215.15	5.51	0.163	0.030	3.16×10^{33}

We examined whether there is a dependence between τ vs. flare amplitude ($f_{\rm amp}$) and τ vs. flare energy ($E_{\rm flare}$). Therefore, we graphically display six panels in Figure 5 showing the relationship between τ and the amplitude of flares and τ and the energy of flares in slow-rotating Sun-like stars 5(a, b), G-type stars 5(c, d) and M-type stars 5(e, f) respectively. In 5(a) for slowly-rotating Sun-like stars, we find that for small amplitude, τ is large, and when the amplitude is large, τ is consistently small in the range considered. The same applies to the relation between τ and energy in Figure 5(b), we see that large τ values correspond to small energies and small values of τ correspond to large energies considered. On the contrary, there is no clear relation between τ vs. $f_{\rm amp}$ and τ vs. $E_{\rm flare}$ in G-type and M-type main sequence stars in Figure 5(c-f). We tried various functions of fit using Python's *curve_fit* and Excel's *trendline*, referred to as a (line of best fit), to visualize the general trend for the data. We could not find any reliable, functional fit dependence between those parameters because *the coefficient of determination*, R^2, which shows how well the data fit the regression model, is less than 0.5 for all those cases in Figure 5(a to f). Hence any attemted fit has been unreliable, as only fit with $R^2 > 0.5$ can be deemed acceptable.

3 CONCLUSIONS

Using our Python script on long cadence data from Data Release 25 (DR 25), we searched for super-flares on main-sequence stars of types (A, F, G, K, and M) based on the entire Kepler data following the method of (Maehara et al. 2012; Shibayama et al. 2013). The Kepler targets' parameters were retrieved from the Kepler Stellar interactive table in the NASA Exoplanet Archive. Using these data, we detected 14 super-flare on 13 Sun-like stars with a surface temperature of $5600K \leqslant T_{\rm eff} < 6000K$, and $P_{\rm rot}$ range from 24.5 to 44 days. In addition, we found 12 and 7 cases of large amplitude super-flares on six and four showed no signs of large-amplitude super-flares. To characterise the flares, we fit an exponential decay function to the flare light curve given by $f(t) = a\ e^{-t/\tau} + b$. We study the relation between the decay time of the flare after its peak τ vs. $f_{\rm amp}$ and τ vs. $E_{\rm flare}$. For slowly rotating Sun-like stars, we find that τ is large for small flare amplitudes and τ is small for large flare amplitudes considered. Similarly, we find that large τ values correspond to small flare energies and small τ values correspond to high flare energies considered. However, for the main sequence stars of the G and M types, τ has no apparent relation to the $f_{\rm amp}$ or $E_{\rm flare}$. We experimented with several different fit functions between τ vs. $f_{\rm amp}$ and τ vs. $E_{\rm flare}$ to better see the underlying pattern in the data. Since the R^2 is less than 0.5 in these cases, we could not identify a reliable fit functional dependence between these parameters.

In conclusion, we believe that:
(i) the thirteen peculiar Kepler IDs that are Sun-like, slowly rotating with rotation periods of 24.5 to 44 days, and yet can produce a super-flare with energies in the range of $(2\text{–}9) \times 10^{34}$ erg; and
(ii) six G-type and four M-type Kepler IDs with exceptionally large amplitude super-flares, with the relative flux in the range $\Delta F/F_{\rm avg} = 4 - 35$;
defy our current understanding of stars and hence are worthy of further investigation.

ACKNOWLEDGEMENTS

Some of the data presented in this paper were obtained from the Mikulski Archive for Space Telescopes (MAST). STScI is operated by the Association of Universities for Research in Astronomy, Inc., under NASA contract NAS5-26555. Support for MAST for non-HST data is provided by the NASA Office of Space Science via grant NNX13AC07G and by other grants and contracts.
Authors would like to thank Deborah Kenny of STScI for kind assistance in obtaining the data, Cozmin Timis and Alex Owen of Queen Mary University of London for the assistance in data handling at the Astronomy Unit.
A. K. Althukair wishes to thank Princess Nourah Bint Abdulrahman University, Riyadh, Saudi Arabia and Royal Embassy of Saudi Arabia Cultural Bureau in London, UK for the financial support of her PhD scholarship, held at Queen Mary University of London.

DATA AVAILABILITY

All data used in this study was generated by our bespoke Python script that can be found at `https://github.com/akthukair/AFD` under the filename AFD.py and other files in the same GitHub repository. The data underlying this article were accessed from Mikulski Archive for Space Telescopes (MAST) `https://mast.stsci.edu/portal/Mashup/Clients/Mast/Portal.html`. The long-cadence Kepler light curves analyzed in this paper can be accessed via MAST STScI (2016). The Kepler Stellar parameters table for all targets can be found at Kepler Mission (2019). The derived data

References

Althukair, A. K., & Tsiklauri, D. 2022, Submitted for publication in Res. Astron. Astrophys., arXiv:2212.10224, doi: 10.48550/arXiv.2212.10224

Caldwell, D. A., Van Cleve, J. E., Jenkins, J. M., et al. 2010, in Space Telescopes and Instrumentation 2010: Optical, Infrared, and Millimeter Wave, Vol. 7731, SPIE, 343–353

Gao, D.-Y., Liu, H.-G., Yang, M., & Zhou, J.-L. 2022, AJ, 164, 213, doi: 10.3847/1538-3881/ac937e

Günther, M. N., Zhan, Z., Seager, S., et al. 2020, The Astronomical Journal, 159, 60

Hawley, S. L., & Fisher, G. H. 1992, ApJS, 78, 565, doi: 10.1086/191640

He, H., Wang, H., & Yun, D. 2015, ApJS, 221, 18, doi: 10.1088/0067-0049/221/1/18

He, H., Wang, H., Zhang, M., et al. 2018, ApJS, 236, 7, doi: 10.3847/1538-4365/aab779

Ilin, E., Poppenhaeger, K., Schmidt, S. J., et al. 2021, MNRAS, 507, 1723, doi: 10.1093/mnras/stab2159

Jackman, J. A. G., Wheatley, P. J., Bayliss, D., et al. 2019, MNRAS, 485, L136, doi: 10.1093/mnrasl/slz039

Katsova, M. M., Kitchatinov, L. L., Livshits, M. A., et al. 2018, Astron. Rep., 62, 72

Kepler Mission. 2019, Kepler Stellar Properties Table, IPAC, doi: 10.26133/NEA6

Kitchatinov, L. L., Mordvinov, A. V., & Nepomnyashchikh, A. A. 2018, Astron. Astrophys., 615, A38, doi: 10.1051/0004-6361/201732549

Kitchatinov, L. L., & Olemskoy, S. 2016, Mon. Not. R. Astron. Soc., 459, 4353

Kretzschmar, M. 2011, A&A, 530, A84, doi: 10.1051/0004-6361/201015930

Lu, H.-p., Zhang, L.-y., Shi, J., et al. 2019, ApJS, 243, 28, doi: 10.3847/1538-4365/ab2f8f

Maehara, H., Shibayama, T., Notsu, S., et al. 2012, Nature, 485, 478, doi: 10.1038/nature11063

Masuda, S., Kosugi, T., Hara, H., Tsuneta, S., & Ogawara, Y. 1994, Nature, 371, 495, doi: 10.1038/371495a0

McIntosh, P. S., & Donnelly, R. F. 1972, Sol. Phys., 23, 444, doi: 10.1007/BF00148107

McQuillan, A., Mazeh, T., & Aigrain, S. 2014, ApJS, 211, 24, doi: 10.1088/0067-0049/211/2/24

Neidig, D. F. 1989, Sol. Phys., 121, 261, doi: 10.1007/BF00161699

Neidig, D. F., & Cliver, E. W. 1983, Sol. Phys., 88, 275, doi: 10.1007/BF00196192

Nogami, D., Notsu, Y., Honda, S. Maehara, H., et al. 2014, Publ. Astron. Soc. Jap., 66, L4, doi: 10.1093/pasj/psu012

Schaefer, B. E., King, J. R., & P., D. C. 2000, Astrophys. J., 529, 1026

Schmidt, S. J., Shappee, B. J., Gagné, J., et al. 2016, ApJ, 828, L22, doi: 10.3847/2041-8205/828/2/L22

Schüssler, M., & Solanki, S. 1992, Astronomy and Astrophysics, 264, L13

Shibata, K., Masuda, S., Shimojo, M., et al. 1995, The Astrophysical Journal, 451, doi: 10.1086/309688

Shibayama, T., Maehara, H., Notsu, S., et al. 2013, The Astrophysical Journal Supplement Series, 209, 5, doi: 10.1088/0067-0049/209/1/5

STScI. 2016, Kepler LC, Q0-Q17, STScI/MAST, doi: 10.17909/T9488N

Tu, Z.-L., Yang, M., Zhang, Z. J., & Wang, F. Y. 2020, ApJ, 890, 46, doi: 10.3847/1538-4357/ab6606

Van Doorsselaere, T., Shariati, H., & Debosscher, J. 2017, ApJS, 232, 26, doi: 10.3847/1538-4365/aa8f9a

VanderPlas, J. T. 2018, ApJS, 236, 16, doi: 10.3847/1538-4365/aab766

Worden, S. 1983, Byrne PB, Rodono M.(Holland: D. Reidel Publ. Co.), 207

Wu, C.-J., Ip, W.-H., & Huang, L.-C. 2015, ApJ, 798, 92, doi: 10.1088/0004-637X/798/2/92

Yang, H., & Liu, J. 2019, ApJS, 241, 29, doi: 10.3847/1538-4365/ab0d28

Yang, H., Liu, J., Gao, Q., et al. 2017, The Astrophysical Journal, 849, 36

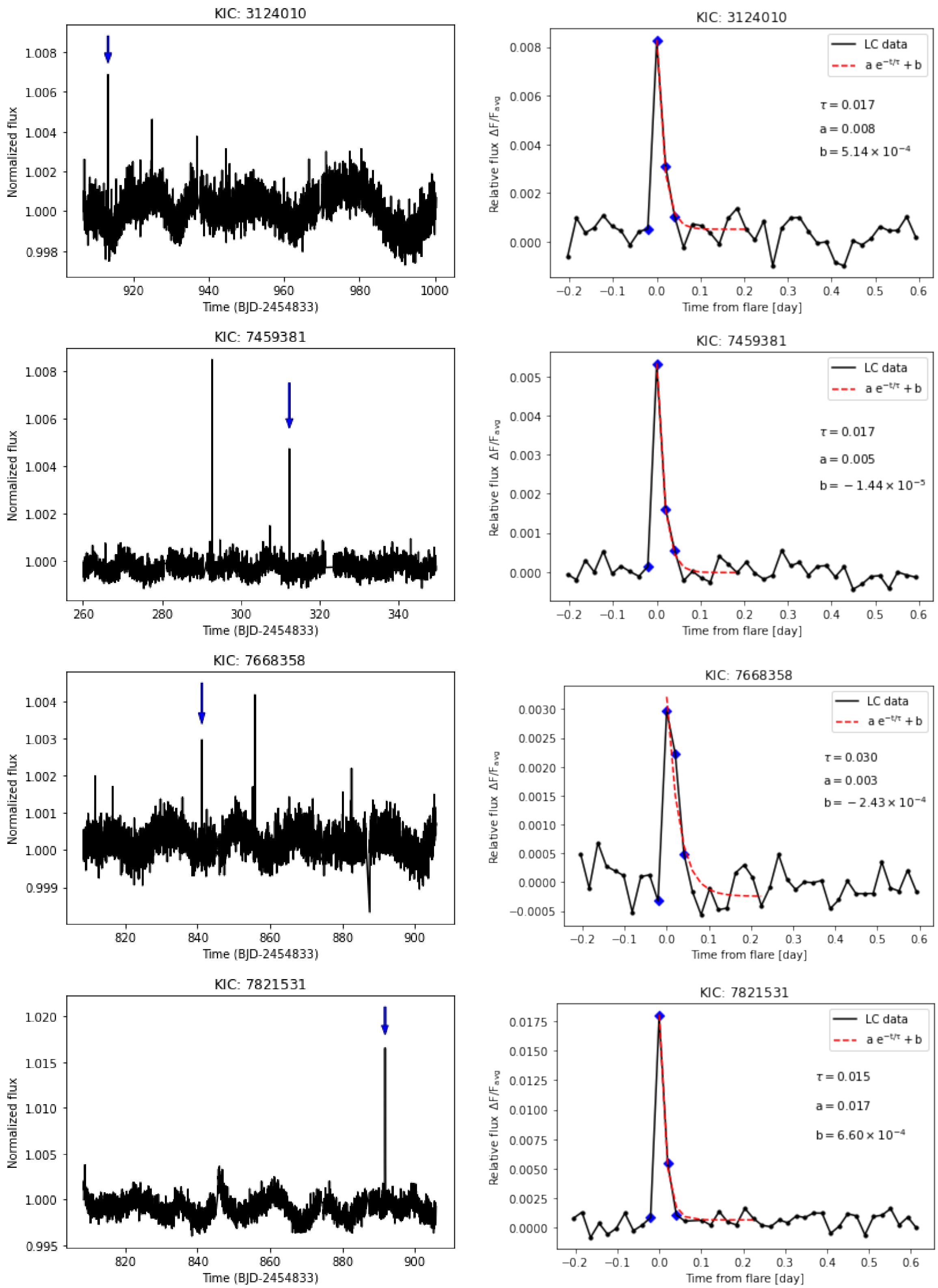

Fig. 2: The left panel displays the light curves of super-flares. The x-axis in the left panel is the time in (BJD) and the y-axis is the normalized flux. The blue arrows indicates the occurrence of super-flares. The right panels show zoom in time of these super-flares. The x-axis in the right panel is the time from the flare peak in (day) and the y-axis is the relative flux ($\Delta F/F_{avg}$). Each data points for a super-flare is represented by blue squares in the right panel. The dashed red curve indicates an exponential fit of the decay phase. τ

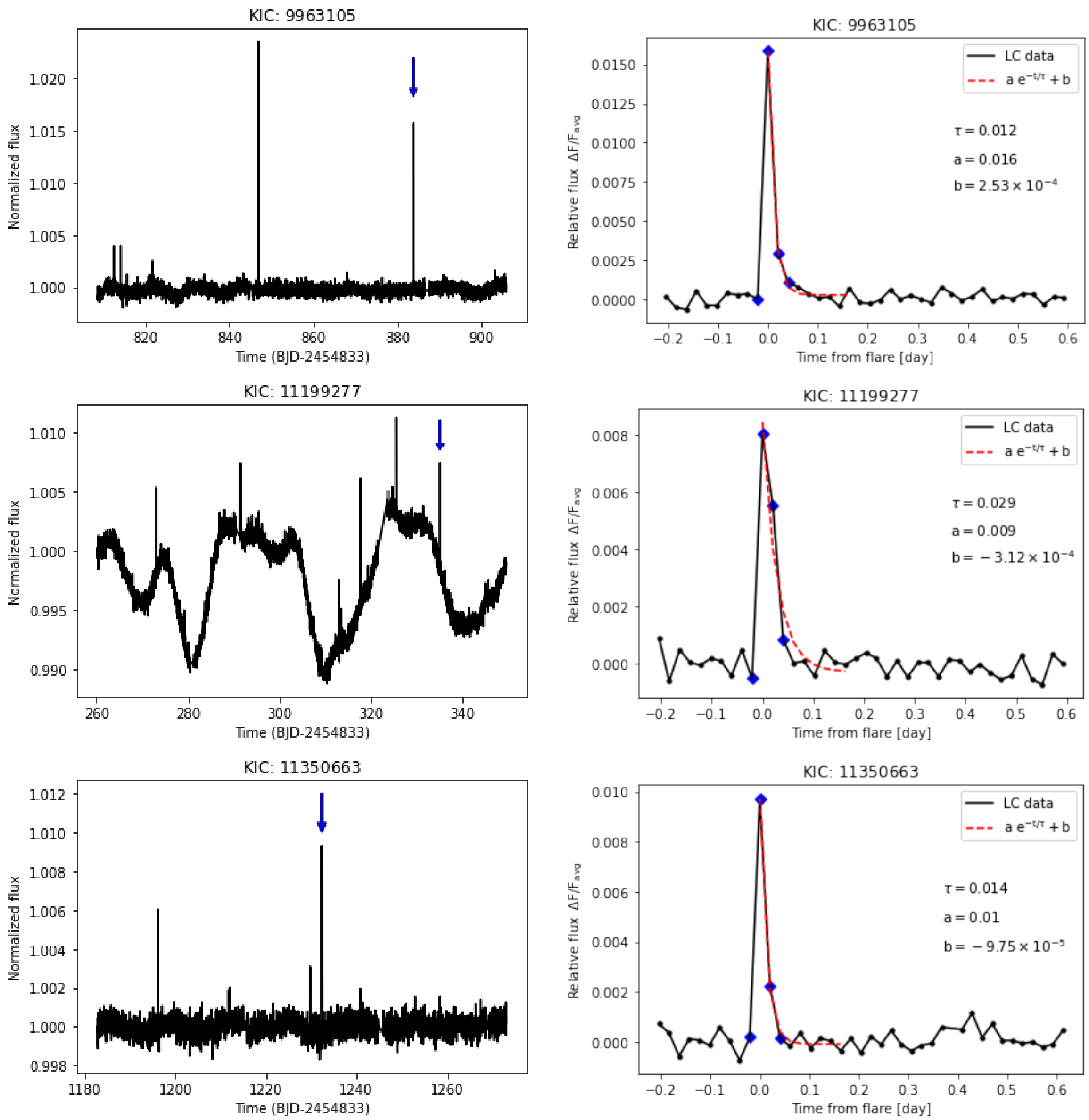

Fig. 2: Figure 2 continued

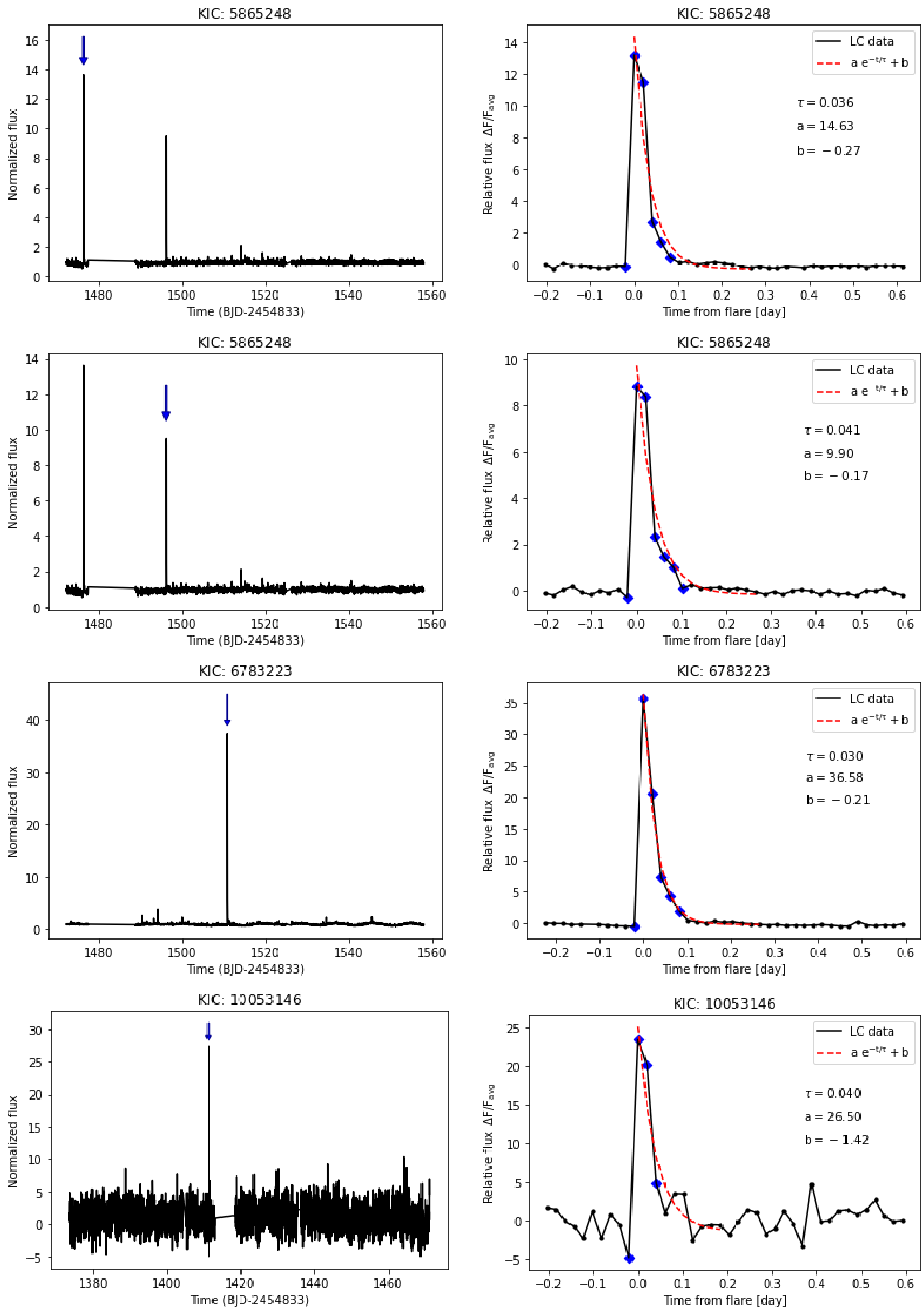

Fig. 3: Same as Figure 2 but for large amplitude super-flares on G-type main-sequence stars.

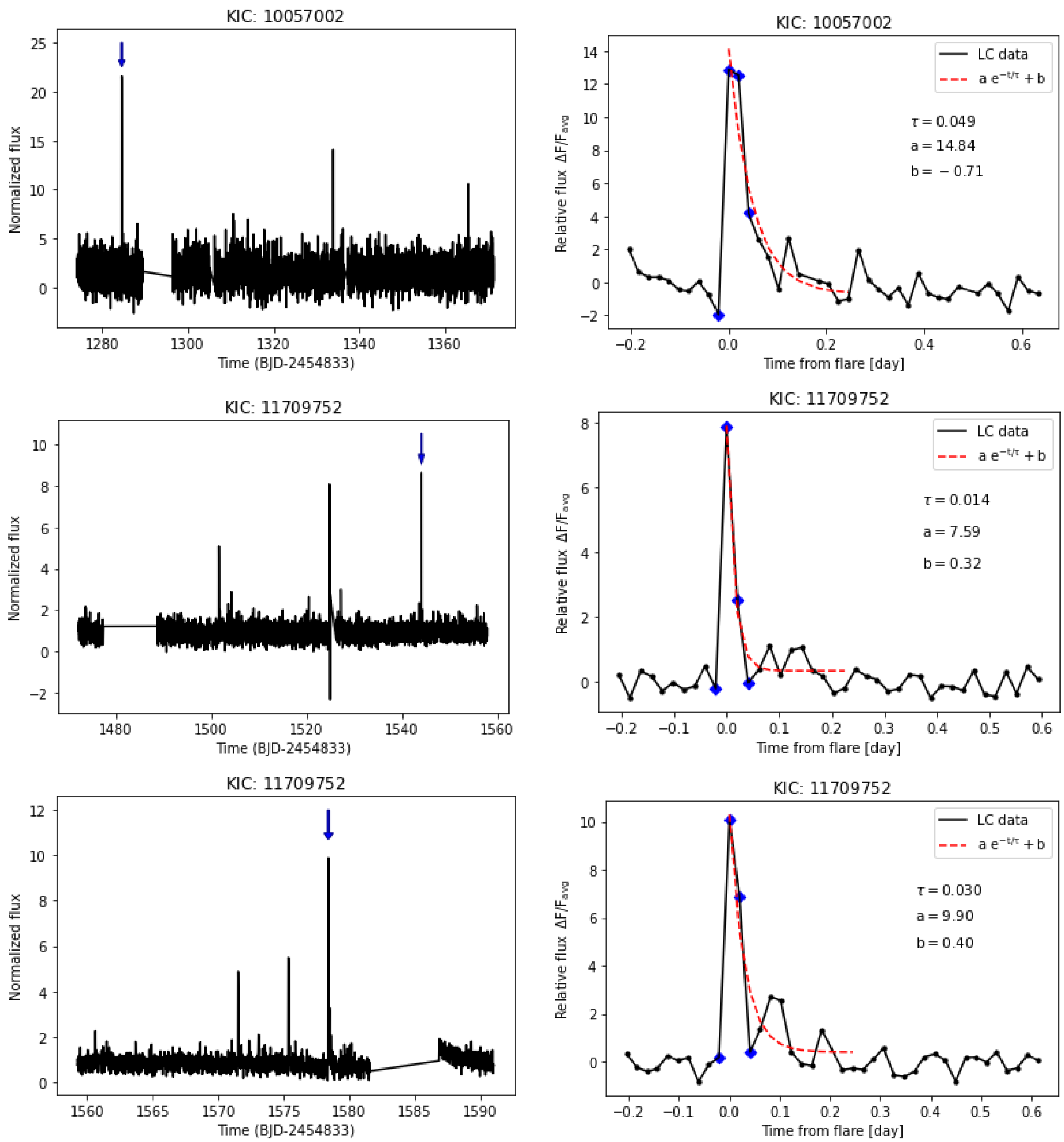

Fig. 3: Same as Figure 2 but for large amplitude super-flares on G-type main-sequence stars

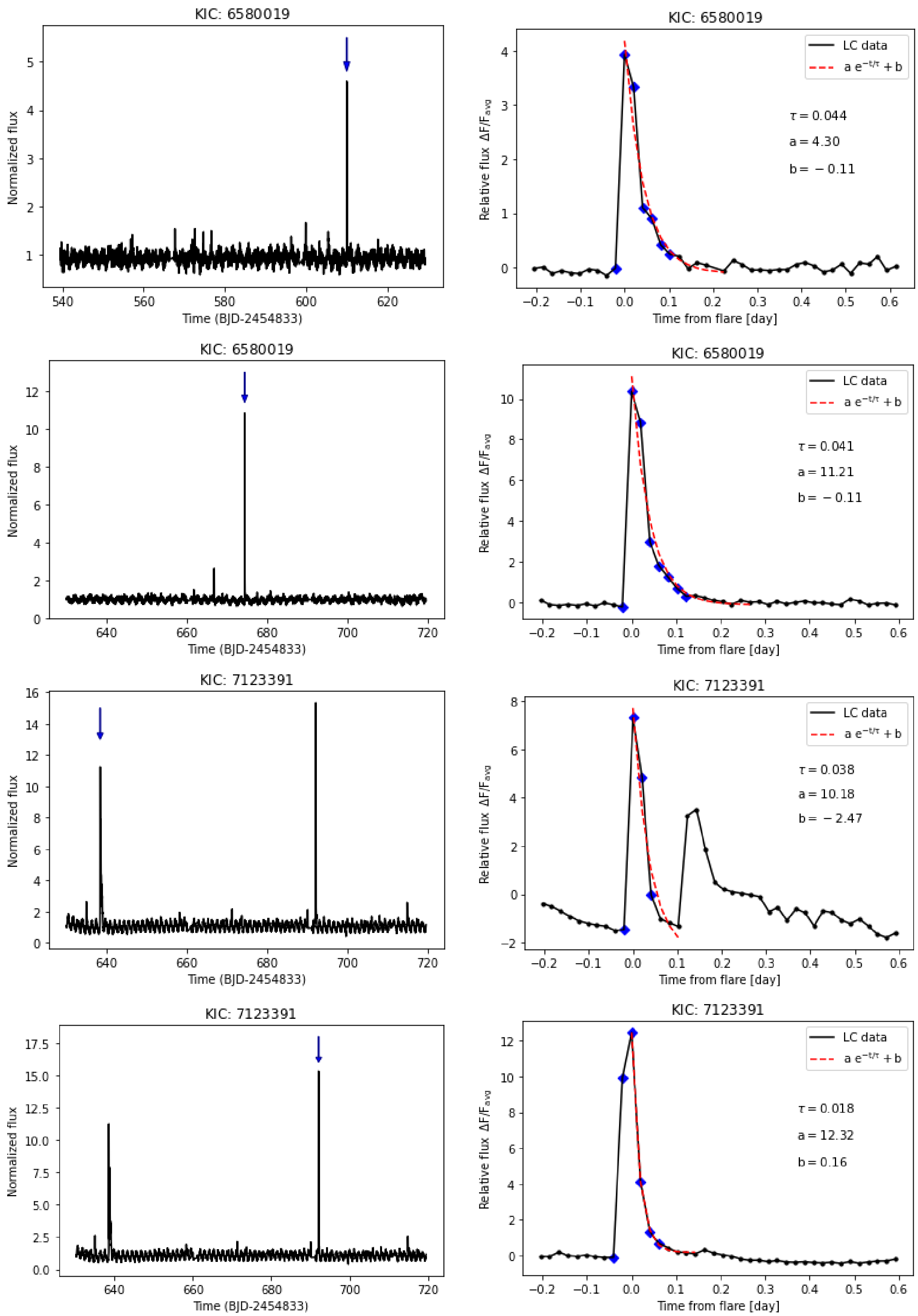

Fig. 4: Same as Figures 2 and 3 but for large amplitude super-flares on M-type main-sequence stars.

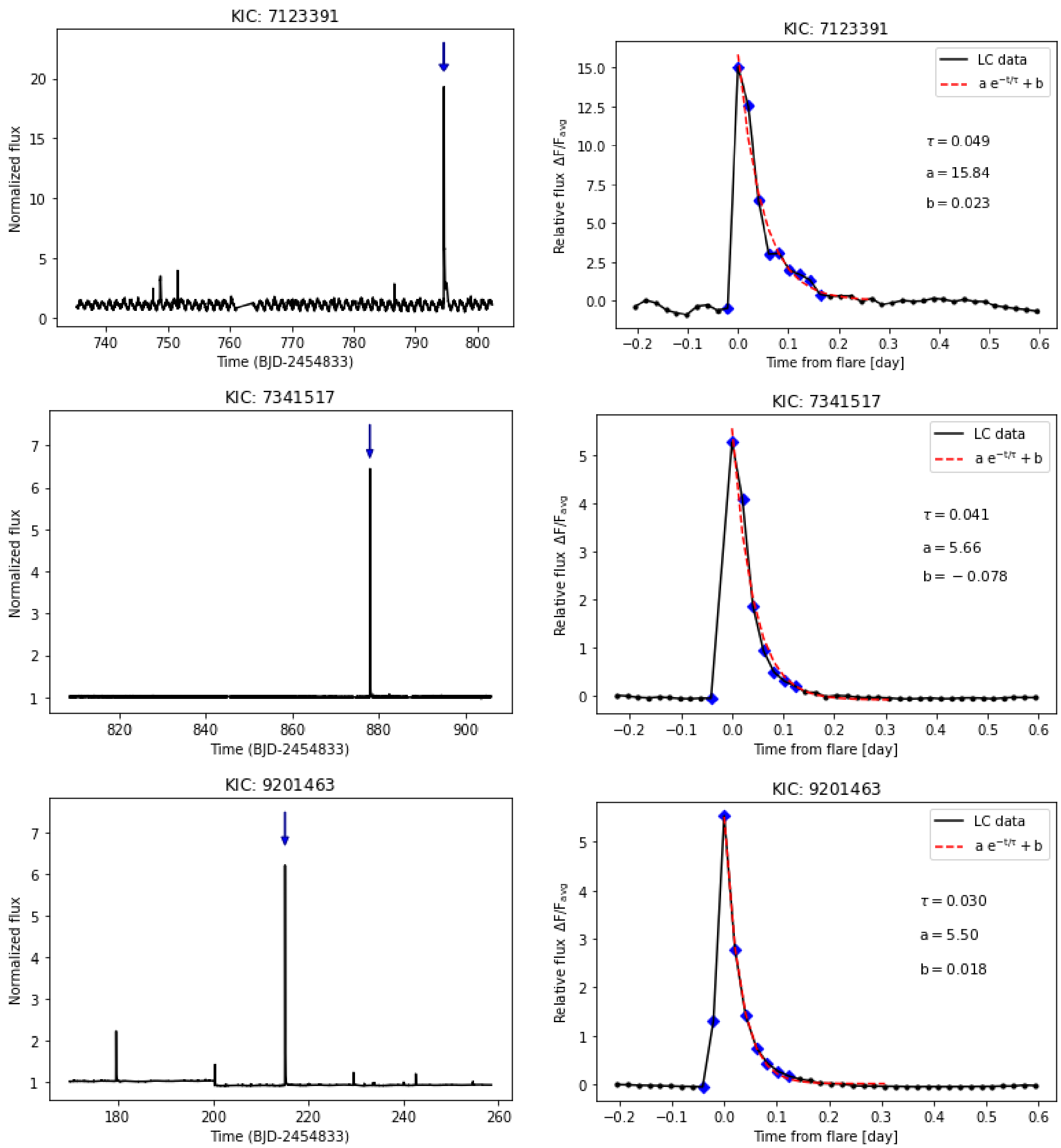

Fig. 4: Same as Figures 2 and 3 but for large amplitude super-flares on M-type main-sequence stars.

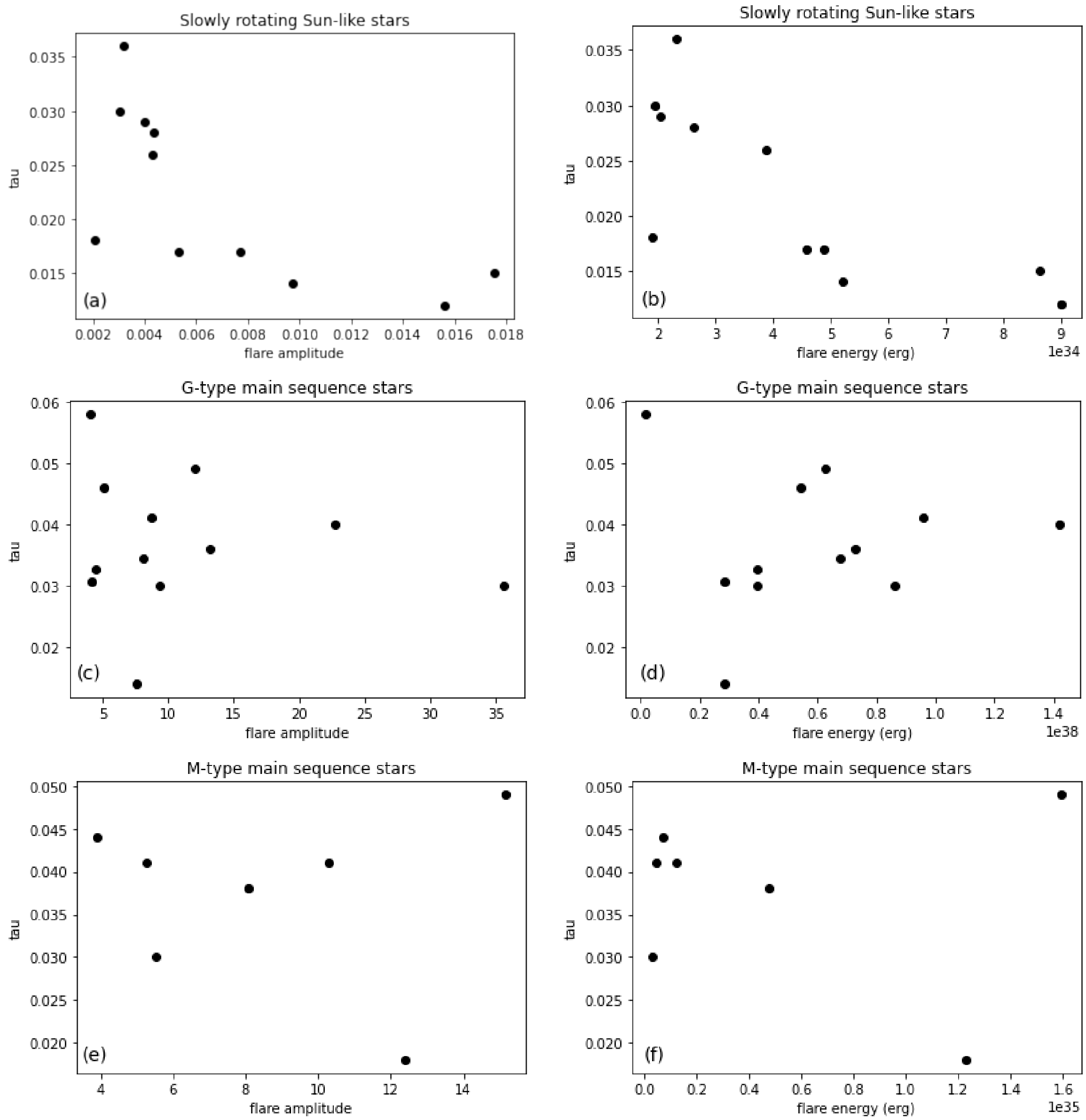

Fig. 5: The left panels display a scatter plot showing the relation between tau values on the y-axis with the flare amplitude f_{amp} on the x-axis. While the right panels display a scatter plot showing the relation between τ values on the y-axis with the flare energy E_{flare} on the x-axis. For flares on slowly rotating Sun-like stars,(a) demonstrates that τ values are large for low flare amplitudes but consistently small for high flare amplitudes. Likewise,(b) demonstrates that high τ values correspond to low flare energies, whereas low τ values correspond to high flare energies. For large amplitude super-flares on G-type dwarfs (c,d) and M-type dwarfs (e,f), τ has no clear connection to the f_{amp} or E_{flare}.